Revue de Chimie minérale,
t. 23, 1986, p. 647

Thermal depolarization phenomena in fluoride solid electrolytes

by

J. SCHOONMAN

Laboratory of Inorganic and Physical Chemistry,
Delft University of Technology,
P. O. Box 5045,
2600 GA Delft, The Netherlands.

ABSTRACT. — Anion-excess solid solutions based on fluorite type metal fluorides, and anion-deficient solid solutions based on tysonite type metal fluorides form good solid electrolytes. The anion-excess solid solutions show a remarkable increase in fluoride interstitial conductivity, while conductivity isotherms of anion deficient solid solutions usually reveal a maximum. The defect structures of these types of solid solutions are dominated by defect association effects, extended defect clustering, ion size effects, and short range ordering. These phenomena often give rise to dielectric relaxation phenomena. The dynamical behaviour of bound ionic defects has been widely studied by Thermally Stimulated (De)Polarization (TSPC, TSDC), and a. c. Dielectric Loss (DL) techniques. Often relaxation of macroscopic space charge, i. e. ionic conductivity, contributes to the dielectric spectra. It will be shown that useful information concerning diffusive ionic motion can be obtained from insight into the dynamical behaviour of bound ionic defects.

RÉSUMÉ. — Les solutions solides de fluorures métalliques à excès anioniques dérivant du type fluorine, et les solutions solides de fluorures métalliques à défauts anioniques dérivant du type tysonite sont de bons électrolytes solides. Les solutions solides à excès anioniques montrent une augmentation remarquable de la conductivité de F^- interstitiel, alors que les isothermes de conductivité de celles à défauts anioniques révèlent généralement un maximum. Les défauts de structure de ces solutions solides sont dominés par des effets de défauts d'association, de défauts étendus de clustering, des effets de dimensions d'ion, et l'ordre à courte distance. Ces phénomènes amènent souvent des phénomènes de relaxation diélectrique. Le comportement dynamique des défauts ioniques a été largement étudié par des techniques de (de)polarisation stimulée thermiquement (TSPC, TSDC) et de perte diélectrique (DL). La relaxation de la conductivité ionique contribue souvent aux spectres diélectriques. Il sera montré que des informations utiles sur la motion ionique diffuse peuvent être obtenues en considérant le comportement dynamique des défauts ioniques.

1. — INTRODUCTION

Metal halides with the fluorite (CaF_2) and tysonite (LaF_3) structure have promising solid electrolyte properties. The defect structure and electrical conductivity of the fluorites with anti-Frenkel disorder CaF_2, SrF_2, BaF_2,

β-PbF_2 and $SrCl_2$ have engaged wide attention, particularily as a result of (i) the discovery of fast ionic conduction in their solid solutions with rare earth fluorides $M_{1-x}RE_xF_{2+x}$ and some tetrafluorides $M_{1-x}Me_xF_{2+2x}$ (Me=Th, U) [1-5], and (ii) the occurrence of ionic conductivities of the order of ionic melts beyond a critical temperature T_c of about 0.8 T_m, where T_m is the melting temperature. It has been shown that this so-called Faraday transition occurs at substantially lower temperatures in these anion-excess solid solutions [6, 7].

Fluorides with the tysonite structure exhibit Schottky disorder, and have electrical properties which are in a number of ways more complex than those with the fluorite structure. In comparison with the fluorite structure, the tysonite structure is more complex in that three different fluoride sublattices can be discerned. This anion array leads to dielectric relaxation phenomena resembling dipolar relaxations of associated defects. Early studies of LaF_3 have shown large polarization effects and relatively fast ionic conduction [8, 9]. Only modest conductivity increases result upon doping tysonites with alkaline earth fluorides. The composition dependence of the ionic conductivity of the anion deficient solid solutions $M'_{1-x}M_xF_{3-x}$ (M'=La, Ce and M=Ca, Sr, Ba) reveals a maximum similar to that observed for anion-deficient fluorite-type oxides like calcia stabilized zirconia. The more recent studies on the tysonites have focused on the conduction mechanism [10-14].

Further research aimed towards optimization of all solid-state electrochemical systems based on these fluoride solid electrolytes is critically dependent on our insights into the mechanism of fast ionic conduction, the relations between chemical composition, defect structures, and optimized ionic conductivity, as well as interfacial polarization phenomena. Especially in these concentrated solid solutions the ionic conductivity is strongly influenced by defect association and clustering phenomena, ion size effects and short range ordering.

While the measurement of electrical conductivity represents a very sensitive technique to investigate ionic transport, other dynamic techniques such as nuclear magnetic resonance (NMR) relaxation, thermal depolarization—ionic thermal current, ITC, and thermally stimulated (de)polarization current, TSP(D)C—and a. c. dielectric relaxation are currently employed to study diffusive and localized motions of point defects in the present solid solutions. In addition, these techniques provide information that contributes to unraveling the defect structures. It is the aim of the present paper to high-light in particular the recent progress made in the

study of localized motions by the thermal depolarization technique in several of these fluorite and tysonite solid electrolytes, and relations with the composition dependence of their ionic conductivities.

2. – THEORETICAL ASPECTS

The Thermally Stimulated Depolarization Current (TSDC) technique, often referred to as Ionic Thermal Current (ITC) technique has become widely used since its introduction in 1964 by Bucci and Fieschi [15]. In practice, ionic thermal currents can be studied in the depolarization (TSDC), or in the polarization (TSPC) mode. In the TSDC mode the sample with bound charge is polarized at a temperature T_p sufficiently high so that the relaxation time τ of the dipoles is short enough for the polarization associated with the dipoles to reach an equilibrium value P_0 in a relatively short time. Then the sample is cooled down to low temperatures, and the external polarization field is switched off. Upon heating at a constant rate the reorienting dipoles cause depolarization currents, which can be analyzed to yield the number of polarizable species, their relaxation times, and their reorientation provided that the dipole moments are known [16]. In the TSPC mode, introduced by Pfister and Abkowitz [17] the dielectric current arising from the sample is recorded when the external electric field E_p is applied at low temperature, and the temperature is then raised with a linear heating rate. The TSPC method allows also the conduction current to be recorded, provided that the sample's electrode contacts are ohmic. Bucci and Fieschi have developed a set of equations describing the depolarization current due to N_d reorienting non-interacting dipoles per unit volume, each with a dipole moment μ, and reorientation energy E. The dipoles reorient with a unique characteristic relaxation time

$$\tau(T) = \tau_0 \exp(E/k\,T) \tag{1}$$

where τ_0 is the characteristic dipole relaxation time. If one has a partially oriented state, at a temperature T, where the sample has a polarization P(T), and is heated with a linear rate b in the absence of an electric field then the depolarization current density is given by

$$I(T) = P_0/\tau_0 \exp(-E/k\,T) \exp\left[-1/b\,\tau_0 \int_0^T \exp(-E/k\,T')\,dT'\right]. \tag{2}$$

For the equilibrium polarization P_0 at the polarization temperature T_p the relation

$$P_0 = \frac{N_d \mu^2 E_p \alpha}{k T_p} \qquad \text{for} \quad k T_p \gg \mu E_p \tag{3}$$

holds, where k is the Boltzmann constant, and α a geometrical factor. For the fluorites α is 1/3 [18] and for the tysonites α is 1/6 [19].

Equation (2) represents an asymmetrical curve. The first exponential dominates in the low-temperature region, and is responsible for the initial increase of the current with temperature, while the second exponential, which dominates in the high-temperature region, slows gradually the current rise down, and subsequently depresses it rapidly. Lenting *et al.* [20], Laredo *et al.* [18], and Roos *et al.* [19] have observed that experimental TSDC spectra and the monoenergetic Bucci and Fieschi theory, i. e. Equation (2) disagree systematically, a disagreement which is well outside the experimental uncertainty. Broadening of the TSDC relaxation peaks as a function of the dipole concentration has been observed by Shelly and Miller [21] in powdered samples of NaF-doped CaF_2, and is ascribed to dipole-dipole interactions. Likewise, it has been found that agreement between experimental and calculated TSDC spectra is greatly improved by assuming a Gaussian distribution of the reorientation energy to account for electrostatic interactions between the dipoles, and contributions from elastic lattice deformations.

A refined approximation to the TSDC equation, taking into account peak broadening by assuming a Gaussian distribution D(E) of width σ has been presented by Laredo *et al.* [18], and Roos *et al.* [19]. If $P(E, T)\,dE$ is the polarization of the sample at temperature T due to dipoles with reorientation energies between E and $E + dE$, than

$$P(E, T)\,dE = P(T)\,D(E)\,dE. \tag{4}$$

Reorientation of these dipoles contributes to the current density at temperature T

$$I(T, E)\,dE = \frac{P(E, 0)}{\tau_0} dE \exp(-E/kT) \exp\left[\frac{-1}{b\tau_0}\int_0^T \exp(-E/kT')\,dT'\right]. \tag{5}$$

The total current density produced by the sample at temperature T can be found by integrating Equation (5), using

$$P_0 = \int_{-\infty}^{+\infty} P(E, 0)\, dE \tag{6}$$

and a Gaussian energy distribution of the form

$$D(E) = \frac{1}{\sigma\sqrt{2\pi}} \exp\left[\frac{-(E-E_0)^2}{2\sigma^2}\right], \tag{7}$$

which yields

$$I(T) = \frac{P_0}{\tau_0 \sigma\sqrt{2\pi}} \int_{-\infty}^{+\infty} \exp(-E/k\,T) \exp\left[\frac{-(E-E_0)^2}{2\sigma^2}\right] \times \exp\left[\frac{-1}{b\,\tau_0} \int_0^T \exp(-E/k\,T')\, dT'\right] dE. \tag{8}$$

Usually experimental TSDC spectra are fitted either to a three-parameter TSDC equation without energy distribution [Equation (2)], or to a four-parameter TSDC equation with energy distribution [Equation (8)] (Laredo *et* la. [18], Roos *et al.* [19]). It has been shown by Roos *et al.* that in the latter case it is sufficient to limit the integration boundaries to $E_0 \pm 5\,\sigma$, which considerably reduces the computing time [19].

In addition to dipolar relaxations the migration of free ionic charge carriers towards the blocking electrodes, i. e. space charge build-up, causes a large TSDC peak to appear. Its relaxation time is controlled by the defect conduction mechanism, and is given by

$$\tau = \frac{\varepsilon\varepsilon_0}{\sigma_i} \tag{9}$$

where σ_i is the ionic conductivity, ε_0 the permittivity of free space, ε the dielectric constant, while for the ionic conductivity the Arrhenius equation

$$\sigma_i = \frac{\sigma_i^0}{T} \exp(-\Delta H_\sigma/k\,T) \tag{10}$$

is used.

Here σ_i^0 contains the concentration of the conducting defects, their charge, the jump distance, the attempt frequency, and the migration

entropy. ΔH_σ represents the migration enthalpy. One now obtains an expression for the temperature of the maximum of this space charge peak T_{max} by differentiating the conventional expression for the depolarization current [Equation (2)], and inserting Equations (9) and (10). The result is [22, 23]

$$\frac{\Delta H_\sigma}{k T_{max}} = \frac{\sigma_i^0}{b \varepsilon \varepsilon_0} \exp\left(- \frac{\Delta H_\sigma}{k T_{max}} \right) + 1. \tag{11}$$

This equation enables the calculation of ΔH_σ from T_{max} data at each composition. The calculated values can then be compared with the experimental values of ΔH_σ from ionic conductivity measurements at elevated temperatures.

Recently, Puma *et al.* [24] have compared the TSDC and TSPC methods. Besides the expression for polarizing current density in the case of zero initial polarization, they present the expression for the polarization when its initial value in nonzero. In particular, they focus attention on current reversals due to the existence of a frozen-in polarization due to processes occurring in the high-temperature part of the dielectric relaxation spectrum. These very interesting phenomena are beyond the scope of this paper.

3. – FLUORITES

The structure of the fluorite (CaF_2) lattice is shown in Figure 1. The structure has a face-centred-cubic translation group and a space lattice of symmetry O_h^5.

Ionic conductivity measurements on fluorites are generally interpreted in terms of a basic model described by Lidiard [25] and Fong [26]. The thermal disorder is generated according to an anti-Frenkel mechanism [26]

$$F_F^x + V_i^x = F_i' + V_F^{\cdot}. \tag{12}$$

Here and throughout this paper the defect notation of Kröger and Vink [27] will be used. Regular lattice ions are represented by F_F^x, and have zero effective charge (x). The anion interstitials F_i' carry an effective negative charge ($'$), while anion vacancies $V_F^{\cdot}$ carry an effective positive charge ($^{\cdot}$). An unoccupied interstitial site is represented by V_i^x. The electrical conductivity results from the migration of anion vacancies and anion interstitials [28]. The indirect or interstitialcy mode of movement of an interstitial anion is given in Figure 2.

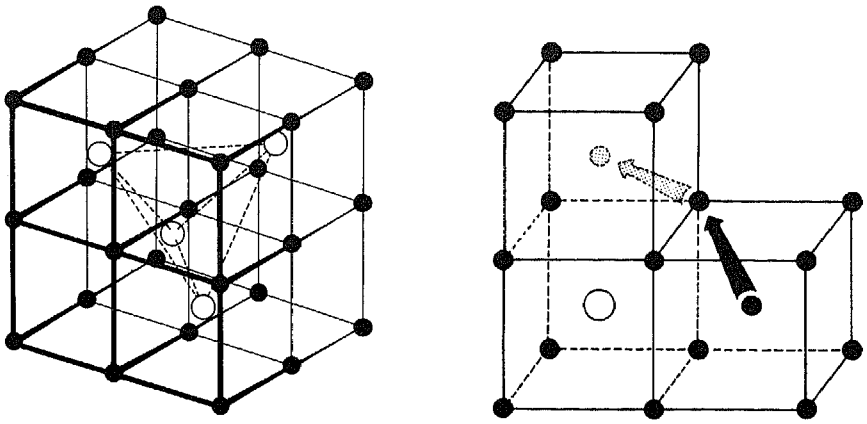

Fig. 1. – The fluorite lattice structure.
Open circles represent cations and solid circles anions.
Fig. 2. – The interstitialcy jump of an interstitial anion.

Anion vacancies exchange with anions at regular lattice sites. At low and moderate temperatures fluoride ion vacancies constitute the more mobile species, while at high temperatures the fluoride interstitials are more mobile [29].

Upon incorporating trivalent rare earth ions RE^{3+} the extrinsic concentration of fluoride interstitials is increased.

$$REF_3 \rightarrow RE_M^{\cdot} + F_i' + 2F_F^x. \tag{13}$$

The defect structure of various complexes between rare earth ions and fluoride interstitials in the dilute solid solutions have been inferred mainly from optical, ESR, and ENDOR studies [28]. For CaF_2, SrF_2 and BaF_2 there exists general consensus as to the presence of simple nearest-neighbour (*nn*, tetragonal symmetry C_{4v}), and next-nearest-neighbour (*nnn*, trigonal symmetry C_{3v}) associates $(RE_M . F_i)^x$. Theoretical and experimental studies have revealed that the ratio of the *nn* to *nnn* associates strongly depends on the lattice parameter of the host lattice: *nn* associates appear to dominate in CaF_2, while *nnn* associates dominate in BaF_2. In SrF_2 the type of associate depends on the size of the rare earth ion, the *nn* associate being present in samples doped with the light rare earths, and *nnn* associates in samples doped with the heavy rare earths. Crawford and Matthews [30] have pointed out that because of the dipolar character an appreciable electrostatic binding between $(RE_M . F_i)^x$ and a mobile F_i' can

be expected. The trapping process can be represented by

$$(RE_M . F_i)^x + F_i' = (RE_M . 2F_i)'. \quad (14)$$

Catlow *et al.* [31] and Jacobs and Ong [32] have calculated the most stable configuration to be an L-shaped complex, while for the binding energy of the additional fluoride interstitial the values 0.4 eV (CaF_2), 0.2 eV (SrF_2), and 0.1 eV (BaF_2) were obtained. When two *nn* associates dimerize to form a square planar configuration, two fluoride lattice ions undergo $\langle 111 \rangle$ displacements, thereby giving the well-known (222) cluster [33]. This cluster arrangment is presented in Figure 3.

Kjems *et al.* [34] have shown that $Ba_{1-x}La_xF_{2+x}$ crystals with $x = 0.209$ and 0.492 show strong anisotropic diffuse neutron scattering which has been explained quantitatively in terms of simple models involving defect clusters of the (222)-type. At low temperature ($T < 400°C$) these clusters are ordered along the (100)-direction in aggregates of up to four (222) clusters. At high temperatures the correlation time between the different (222) clusters in the aggregates is slowly lost. The implications for the conduction processes have recently been discussed [34, 35].

The neutral associate $(U_M . 2F_i)^x$ would induce coupled lattice interstitial relaxations, which could also lead to the vacancy interstitial configuration of the (222) cluster [1]. This so-called (212) cluster has recently been observed in quasi-elastic neutron scattering experiments on $Ba_{1-x}U_xF_{2+2x}$ single crystals [36, 37]. Figure 4 presents the (212) cluster arrangement.

Since the pioneering work of Cheetman *et al.* [33] and Catlow [38] many groups have studied defect clustering in rare-earth doped alkaline earth fluorides. Direct observations of the dopant environments in fluorites using extended X-ray absorption fine structure has recently been reported by Catlow *et al.* [39]. The local structural environment of the dopant alters with the size of the rare earth ion. Because much of the research has been performed independently, a wide variety of notations exists. Andeen *et al.* [40] have recently reviewed existing notations. A systematic notation for defect clusters has recently been put forward by Corish *et al.* [41] and Bendall *et al.* [42]. A cluster is described by the symbol $i/v/p/q_r s_t \ldots$, where i denotes the number of substitutional impurity ions, v the number of vacancies, p the number of relaxed lattice ions, q the number of *nn*-interstitials ($r = 1$), and s the number of *nnn*-interstitials ($t = 2$). The (222)-cluster structure is catalogued as a $2/0/2/2_1$ cluster. It should be emphasized that this notation distinguishes between a vacancy and a vacant site resulting from a relaxed lattice ion. Andeen *et al.* [40] have

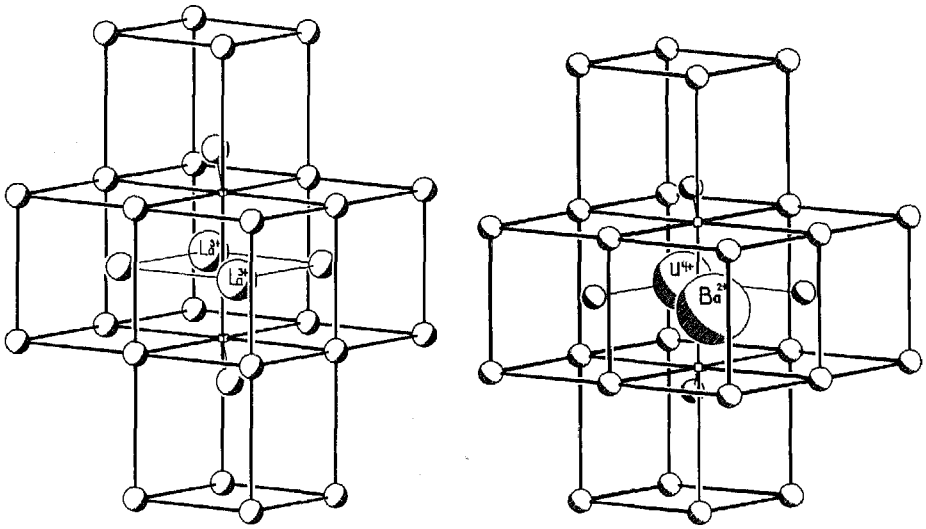

Fig. 3. — A (222) cluster in $Ba_{1-x}La_xF_{2+x}$ solid solutions.
Fig. 4. — A (212) cluster in $Ba_{1-x}U_xF_{2+2x}$ solid solutions.

found evidence for a complex comprising the usual (222) configuration plus an extra fluoride interstitial. In this so-called "gettered" (222) cluster ($2/0/2/3_1$) the extra interstitial can be situated in one of the empty cubes along a (100) direction from one of the rare earth dopant ions in the (222) cluster. In addition to the (212) cluster ($1/0/2/2_1$) Matar *et al.* [43] predicted the presence of a different type of defect cluster in $Ca_{1-x}U_xF_{2+2x}$. This defect cluster comprising one dopant ion, three fluoride ion interstitials, and one fluoride ion vacancy ($1/0/1/3_1$) is called a trimer (viz. Figure 5).

The thermal depolarization phenomena of the dilute anion-excess solid solutions $M_{1-x}RE_xF_{2+x}$ have been studied in great detail by many research groups. Some numerical values are gathered in Table I.

TABLE I

Reorientation energies E *and migration enthalpies* $\Delta H_m,F_i'$ *for selected anion excess solid solutions.*

Solid solution	E_m	E_{mm}	$\Delta H_m,F_i'$
$Ca_{1-x}La_xF_{2+x}$	0.475	—	0.79
$Ba_{1-x}La_xF_{2+x}$	0.391	0.544	0.714
$Ba_{1-x}Y_xF_{2+x}$	0.45	0.56	0.714
$Sr_{1-x}La_xF_{2+x}$	0.444	—	0.74

For all solid solutions the following trend is noted

$$E_{nn} < E_{nnn} < \Delta H_{m,F_i'}.$$

These results indicate that the bound motion of fluoride interstitials via an interstitialcy mechanism (viz. Figure 2) is greatly perturbed by the presence of lattice disturbing defects.

With increasing dopant content defect clustering occurs as described above. Yet the ionic conductivity increases exponentially, while the conductivity activation enthalpy linearly decreases [1]. Based on the trends given

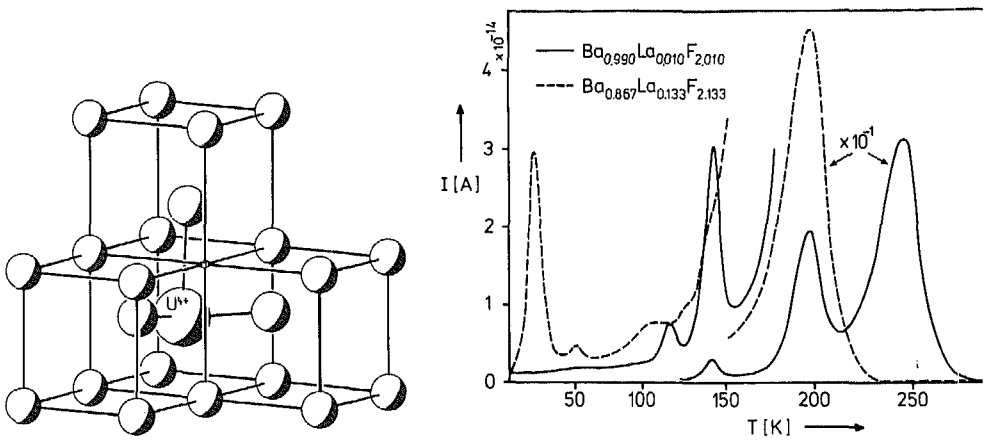

Fig. 5. — A trimer in $Ca_{1-x}U_xF_{2+2x}$ solid solutions.
Fig. 6. — TSDC spectra of $Ba_{1-x}La_xF_{2+x}$ solid solutions.

in Table I, these conductivity effects have been accounted for in an Enhanced Ionic Motion (EIM) model: due to the presence of a large number of lattice disturbing defect clusters, a broad distribution of interstitial defect jumps with slightly different activation enthalpies governs the conduction mechanism. Taking a Gaussian distribution function, the conductivity equation becomes

$$\sigma T = \sigma^0 \exp\left[-\frac{1}{kT}\left(\overline{\Delta H}_m - \frac{p^2}{4kT}\right)\right]. \tag{15}$$

The conductivity activation enthalpy is given by

$$\Delta H = \overline{\Delta H}_m - \frac{p^2}{4kT}. \tag{16}$$

Here $\overline{\Delta H}_m$ is the average value of ΔH, and p the width of the interaction energy distribution function. Agreement with experiment is obtained with "monopole-monopole" interactions, i. e. mobile – immobilized interstitial [3]. In the more concentrated solid solutions complex TSDC spectra occur. The TSDC spectra of two $Ba_{1-x}La_xF_{2+x}$ solid solutions are presented in Figure 6.

The peak with T_{max} at 245 K is due to the relaxation of macroscopic space charge. T_{max} shifts to lower temperature for increasing dopant content. The dipolar relaxations at 141 and 195 K are ascribed to *nn*- and *nnn*-associates, respectively [23]. For the concentrated solid solution the peaks at 117 and 21 K have been fitted to a four-parameter TSDC equation to yield for E the values 0.28 and 0.061 eV, respectively, and for τ_0 the values 1.2×10^{-10} s, respectively 1.0×10^{-13} s. The former peak is ascribed to the reorientation of an L-shaped complex $(La_{Ba}.2F_i)'$, and the latter peak to a depolarization step in the (222) cluster [23, 44]. In the concentrated solid solution the space charge peak at 190 K completely masks the *nn*- and *nnn*-dipolar relaxations. The concentration dependence of the space charge T_{max} closely resembles that of the conductivity activation enthalpy, as is expected from Equation (11) [3, 7, 45]. From TSPC spectra Wapenaar [2] calculated low-temperature ionic conductivities which extrapolate to high-temperature a. c. ionic conductivities, thus confirming the relaxation of macroscopic space charge to be a conduction phenomenon.

A possible reorientation mechanism in a (222)-cluster has been proposed by Jacobs and Ong [32] in their TSDC-study of $Ca_{1-x}Y_xF_{2+x}$ solid solutions. By this mechanism the polarizing step is a shift of the relaxed fluoride ions above and below the plane of the cluster from a *trans* to a *cis* (222)-configuration. The depolarization step in the TSDC spectrum comprises a *cis* to *trans* relaxation. The depolarization path will lead a negatively charged fluoride interstitial through an effectively positive vacant anion site to an empty interstitial site (viz. Figure 7).

The reorientation parameters of the L-shaped and (222)-cluster arrangements are concordant with the trends in Table I.

The results of TSDC measurements on two different $Ba_{1-x}U_xF_{2+2x}$ solid solutions are presented in Figure 8.

The most prominent feature is a relaxation peak at 29.5 K, which is present in both dilute and concentrated solutions. A fit to the four-parameter TSDC equation yields for E values in the range 0.089 6 to 0.090 5 eV. The broadening parameter increases from 0.001 4 to 0.008 9 eV.

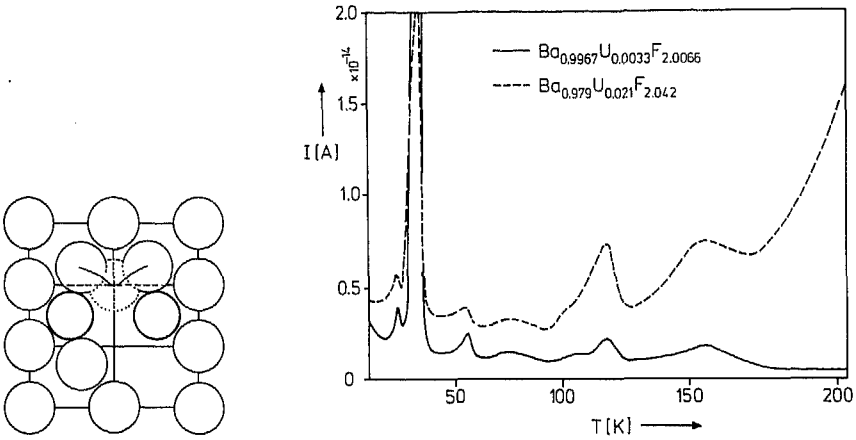

Fig. 7. — The (de)polarization step in a (222) cluster in $Ba_{1-x}La_xF_{2+x}$.
Fig. 8. — TSDC spectra of $Ba_{1-x}U_xF_{2+2x}$ solid solutions.

For τ_0 the value 8×10^{-14} s is obtained. This relaxation is ascribed to a (212)-cluster. Because this cluster contains only one dopant ion it is formed wherever a $(U_{Ba} . 2F_i)^x$ associate is formed. The most plausible polarization of a (212) cluster comprises the shift of the two relaxed ions from the *cis* configuration above and below the U^{4+} ion to a *cis* configuration with both interstitials above and below the lattice Ba^{2+} ion [44].

An important factor to note for the interpretation of the TSDC results is the immobility of the dopant cations in the fluorite lattice. A (212) cluster has therefore much more freedom of orientation than a (222)-cluster. In a (212)-cluster the two fluoride ion interstitials can "connect" a U^{4+} ion with a Ba^{2+} ion in twelve different directions. All directions yield equivalent (212) clusters.

On the contrary a (222)-cluster is fixed in one position because of the connected La^{3+} ions. Only the relaxed ions above and below the plane of the cluster have the ability to reorient. In $Ba_{1-x}U_xF_{2+2x}$ another reorientation process, dependent on the direction of the polarizing field can be envisaged. A polarizing field along the $(\overline{1}\overline{1}\overline{1})$ direction causes a polarized state of a (212)-cluster with a dipole moment opposing the electric field, i.e. in the (111) direction. This configuration is the trimer configuration presented in Figure 5. A trimer with a dipole moment in the (111) direction can be formed from (212)-clusters with a dipole moment in the (110), (101), and (011) direction in a single step. To polarize a (212)-cluster with its dipole moment in the $(\overline{1}\overline{1}0)$ direction to a trimer with its dipole moment in the (111) direction takes three steps [46]. The subsequent depolarization

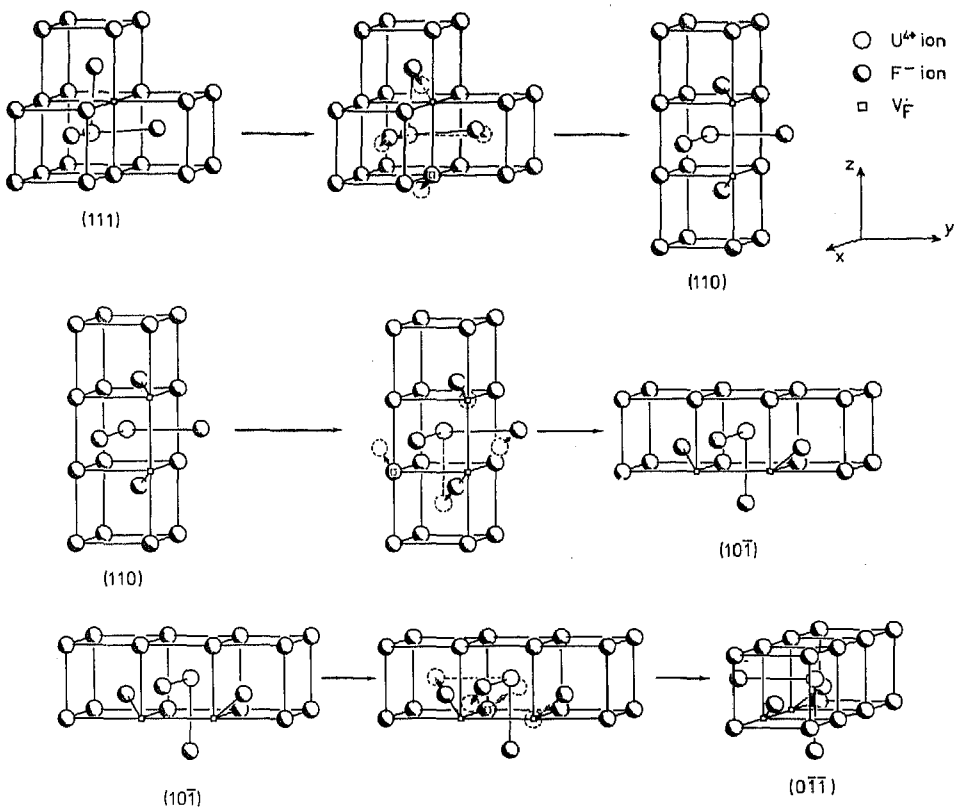

Fig. 9. The three reorientation steps which depolarize a trimer, having its dipole moment in the ($\bar{1}\bar{1}1$) direction, to a (212) cluster with its dipole moment in the (0$\bar{1}\bar{1}$) direction.

steps are depicted in Figure 9. The first step, from a trimer with its dipole moment in the (111) direction to a (212)-cluster with its dipole moment in the (110) direction consists of only small and practically unhindered displacements of four fluoride ions. The activation energy for this reorientation will probably be so low that this trimer depolarization will already take place at liquid helium temperature when the electric field is switched off. Hence the reorientation energy will be less than 0.04 eV.

The second and third depolarization steps in Figure 9 are indentical, and will require the same activation energy. Hence, they will both contribute to the depolarization current. The reorientation peak at 29.5 K for the $Ba_{1-x}U_xF_{2+2x}$ solid solutions has a computed activation enthalpy of 0.09 eV and represents the most prominent dipolar feature in the TSDC

scan. The 29.5 K peak has been assigned to these $(110) \rightarrow (10\bar{1})$, and $(10\bar{1}) \rightarrow (0\bar{1}\bar{1})$ reorientations.

The TSDC spectra of $Ba_{1-x}U_xF_{2+2x}$ solid solutions reveal six relaxations in addition to the large peak at 29.5 K. It was reported that during crystal growth reduction of a small fraction of U^{4+} to U^{3+} was likely to occur [44]. With trivalent uranium *nn*- and *nnn*-associates $(U_{Ba}F_i)^x$ can be formed. The depolarization activation energies of the peaks at 119 and 155 K were found to be concordant with data reported for *nn*- and *nnn*-associates in the solid solutions $Ba_{1-x}U_xF_{2+2x}$ [47]. The other small peaks are to be related with other residual impurities of which the nature has not been established.

The space charge peak in $Ba_{1-x}U_xF_{2+2x}$ has been studied as a function of x. The variation of T_{max} with x is very similar to the variation of the conductivity activation enthalpy with x. Equation (11) has been used to calculate enthalpy data from T_{max}. The results are gathered in Table II.

The agreement is very satisfactory. Also for this type of solid solution space charge relaxation is due to ionic conduction.

TABLE II

$\Delta H_{\sigma,TSDC}$ *compared with* $\Delta H_{\sigma,cond}$ *for* $Ba_{1-x}U_xF_{2+2x}$.

x	$\Delta H_{\sigma,TSDC}$	$\Delta H_{\sigma,cond}$
0	1.440	1.35
0.009	1.244	1.13
0.012	1.137	1.07
0.018	1.007	1.00
0.021	0.935	0.98
0.03	0.761	0.79
0.055	0.639	0.64
0.113	0.549	0.536
0.168	0.506	0.493

4. – TYSONITES

The structure of the tysonite (LaF_3) lattice is shown in Figure 10. Although there is still some disagreement concerning the exact lattice structure of LaF_3, the weight of recent evidence favours a trigonal structure of space group $P\bar{3}Cl\text{-}D^4_{3d}$, in which there are three fluoride sublattices,

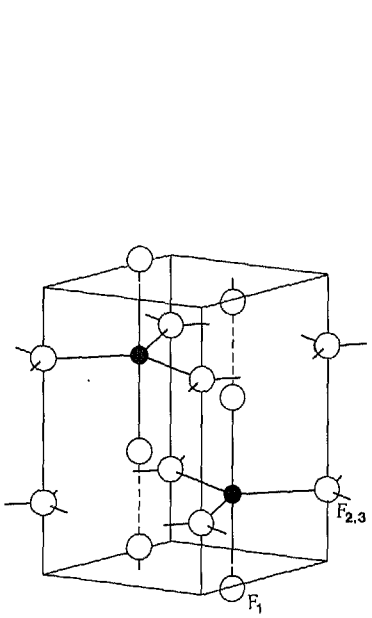

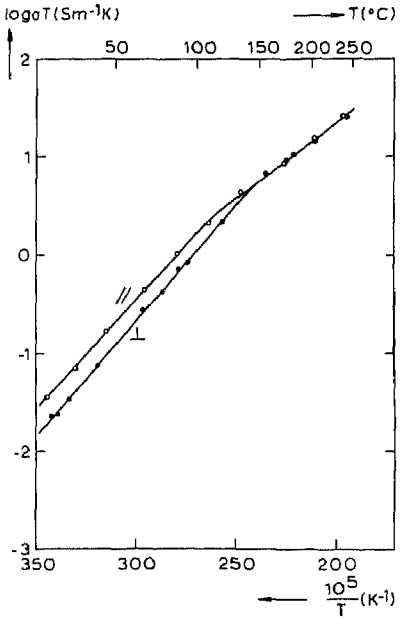

Fig. 10. — The tysonite structure. Open circles represent anions and solid circles cations.
Fig. 11. — Extrinsic conductivity of nominally pure LaF_3 [29].

which contain fluoride sites in the ratio 12 : 4 : 2. The F_2 and F_3 sites are, however, almost indentical in environment, and cannot be distinguished in ^{19}F NMR experiments [11].

Fairly extensive studies of the small-signal a. c. response of LaF_3 and $La_{1-x}Ba_xF_{3-x}$ have appeared [12, 19, 48]. It is generally believed that the intrinsic point defects in LaF_3 are thermally generated according to a Schottky mechanism. The transference number of the fluoride ions is unity. Hence, the ionic transport is governed by the fluoride ion vacancies. The incorporation of alkaline earth fluorides is described by

$$MF_2 \rightarrow M'_{La} + V_F^{\cdot} + 2F_F^x. \tag{17}$$

The temperature dependence of the extrinsic bulk ionic conductivity of LaF_3 and the anion-deficient solid solutions reveals a knee, suggesting a change-over from a classical defect dipole dissociation mode: $(M_{La} \cdot V_F)^x \rightarrow M'_{La} + V_F^{\cdot}$ to a free defect conduction mode: $V_F^{\cdot}$. This behaviour is exemplified in Figure 11.

The anisotropy has been related with the different types of anion site. Thermally stimulated (de)polarization have been reported for solid

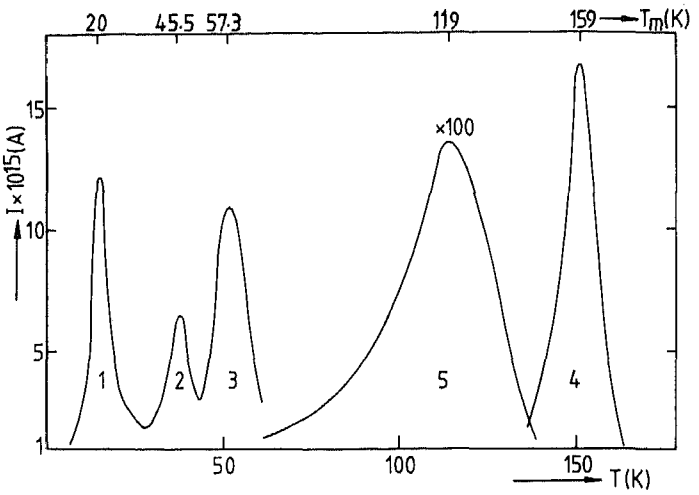

Fig. 12. — TSDC spectrum of $La_{1-x}Ba_xF_{3-x}$ ($x=0.0126$).

solutions $La_{1-x}Ca_xF_{3-x}$ [49] and $La_{1-x}Ba_xF_{3-x}$ [48]. In the former solid solution one dipolar peak, and a space charge relaxation were detected, while in the latter solid solution at least two dipolar and a space charge relaxation showed up in the region 80 to 300 K. From 5 to 80 K three relaxations were observed for $La_{1-x}Ba_xF_{3-x}$ [19, 48, 50], which are probably due to rare-earth impurities in the starting LaF_3 material. A TSDC spectrum is presented in Figure 12.

The spectra have been analyzed with the four-parameter TSDC formula to yield accurate relaxation parameters (viz. Table III). In the nominally pure LaF_3 crystals two dipolar peaks occur at 114 and 153 K. In the solid solutions the space charge peak [5] masks the dipole relaxation at 114 K.

The relaxation parameters for this latter peak are $E=0.30$ eV, $\tau_0=2.5\times10^{-12}$ s, $\sigma=0.56\times10^{-2}$ eV. For the nominally pure material the conductivity activation enthalpies are 0.46 and 0.43 eV, while for the solid solutions values between 0.36 and 0.40 eV are found [19]. Minor differences between conduction and reorientation enthalpies are to be expected only when the size of the solute ion matches that of the host lattice cation [51].

Fontanella *et al.* [51], and Igel *et al.* [13] have studied the relation between free and bound ion motion in $La_{1-x}Ca_xF_{3-x}$ using audio-frequency complex impedance measurements. At five audio-frequencies in the range 10^2 to 10^4 Hz values were measured for the complex dielectric

TABLE III

Relaxation parameters for $La_{1-x}Ba_xF_{3-x}$ as obtained by a fit to Equation 8.

	T_m(K)	τ_0(s)	E(eV)	σ(eV)	$x_m(m/0)$(*)	$x_w(m/0)$(**)
1	20.3	$.34\cdot10^{-11}$	.01	.012	–	–
2	45.5	$.11\cdot10^{-8}$	.15	.038	–	–
3	57.7	$.18\cdot10^{-9}$	.11	.27	–	–
4	153	$.62\cdot10^{-12}$	.50	$.49.10^{-2}$	.01	2.73

(*) Relative amount of dipoles present in mole percent ($m/0$).
(**) Relative amount of Ba^{2+} ions present in $m/0$.

constant $\varepsilon^* = \varepsilon' - j\omega\varepsilon''$, and the results were transformed to the conductivity using $\sigma = \varepsilon_0 \varepsilon'' \omega$. The following equation was then best fitted to the data

$$\sigma T = \sigma^0 \exp(-\Delta H/k T) + \frac{\varepsilon_0 \omega A \cos(\alpha\pi/2)}{2\{\cosh[(1-\alpha)x] + \sin(\alpha\pi/2)\}}. \quad (18)$$

The first term describes the high-temperature bulk ionic conductivity [Equation (10)]. The conductivity activation enthalpy ΔH represents $\Delta H_\sigma + 1/2\,\Delta H_d$, where ΔH_σ represents the vacancy migration enthalpy, and ΔH_d the dissociation enthalpy of the associates $(Ca_{La} . V_F)^x$.

The second term in Equation (18) is the Cole-Cole expression [52] where $x = \ln(\omega\tau)$ and τ is given by Equation (1). A is the dipole strength, and α is a measure for the frenquently observed broadening of the relaxation peaks. At low temperatures dipolar relaxation superimposed on the bulk ionic conductivity shows up in the Arrhenius plot of the monofrequency conductivity.

It should be borne in mind that a TSDC experiment can be regarded as a DL experiment ($\varepsilon'' - T$) at an extremely low measuring frequency [53]. The equivalent frequency of a TSDC experiment can be obtained by differentiating Equation (2) with respect to temperature,

$$f_{eq} = \omega_{max}/2\pi = \frac{1}{2\pi\tau_{max}} = b\,E/2\pi k\,T^2_{max}. \quad (19)$$

For a typical TSDC experiment $b = 0.07$ K/s. f_{eq} then varies from about 2 to 3 mHz for T_{max} variations from about 150 to 110 K, i. e. frequencies

which are much lower than those normally employed in a. c. DL measurements. Relaxation data obtained with both techniques, therefore, cover a wide frequency regime, typically six orders of magnitude. Roos *et al.* [19] have reported the combination of TSDC and DL measurements for the system $La_{1-x}Ba_xF_{3-x}$. The DL data for the system $La_{1-x}Ca_xF_{3-x}$ [13, 51] using a data analysis based on Equation (18) reveals the reorientation energy E of the bound vacancy in the dipole $(Ca_{La}.V_F)^x$ to be close to the vacancy migration enthalpy for diffusive motion in $La_{1-x}Ca_xF_{3-x}$. However, the values of τ_0 in the bulk ionic conductivity term of Equation (18) do not vary with the square root of the solute content as is to be expected if substantial association between Ca'_{La} dopant ions and fluoride ion vacancies $V_F^{\cdot}$ has occurred.

In the system $La_{1-x}Ba_xF_{3-x}$ the relative amount of dipoles turned out to be small compared to the solute content (viz. Table III). This amount of dipoles is too small to be noticed in the ionic conductivity as a dissociation regime. We now turn to the fact that in the tysonite structure different types of anion site exists. This means that the anion conductivity cannot be interpreted in terms of a single thermally activated jump probability. Even if we treat the F_2 and F_3 sites equivalent, at least three different anion jumps are possible: F_1-F_1, F_1-$F_2(F_3)$, $F_2(F_3)$-$F_2(F_3)$.

Recently Franceschetti and Shipe [54] have developed a general model to account for the small-signal a. c. response of tysonite-type materials taking two different sublattices in the anion array into account.

This model has recently been applied to analyze experimental bulk a. c. response data for $La_{1-x}Ba_xF_{3-x}$ with ionically blocking electrodes in the frequency range 10^{-2} to 10^5 Hz and for temperatures from 300 to 1,300 K [19, 48]. In the lower "association" part of this temperature region most of the data could be fitted to a Debye-type equivalent circuit. The model, however, does not require the presence of dipolar complexes. Instead, the Debye-type circuit elements are associated with a macroscopic polarization of the material due to the distribution of anion vacancies on two different sublattices. A detailed description of this model is beyond the scope of this paper.

At room temperature the F_2 type ions are moving much faster than the F_1 ions. In undoped LaF_3 the a. c. conductivity is governed by vacancies in the $F_2(F_3)$ anion array. In undoped LaF_3 exchange between $F_2(F_3)$ and F_1 sites does not occur. This exchange does increase with increasing temperature, but also with increasing dopant concentration [50] as has been demonstrated with ^{19}F NMR [55]. This exchange has a pronounced

influence on the conductivity activation enthalpies. A combination of structural, and mobility arguments has been used to assign the dipolar relaxation at 114 K to an *nn*-associate $(Ba_{La}V_F)^x$ with a vacancy on the $F_2(F_3)$ array, and the dipolar relaxation at 153 K to an *nn*-associate $(Ba_{La}.V_F)^x$ with a vacancy on the F_1 array. The detailed reorientation pathways taking the different jump probabilities into account have been described recently. It appears that in describing the dynamical behaviour of bound vacancies exchange restrictions are less severe than in the case of the a. c. bulk ionic conductivity [19].

By using non-blocking electrodes the ionic conductivity contribution to the TSPC spectra has been separated from contributions due to localized relaxations. Usually the localized relaxations are polarized first. The subsequent TSPC run with the same polarizing field yields then only the non-blocked ionic current [56]. For the system $La_{1-x}Ba_xF_{3-x}$ TSPC conductivity data recored in the temperature region 180 to 250 K extrapolate to high-temperature a. c. bulk ionic conductivity data.

For the fluorite-type anion-excess solid solutions $M_{1-x}RE_xF_{2+x}$ the conductivity activation enthalpies linearly decrease with x. The composition dependence of T_{max} of the space charge peak exhibits a similar behaviour.

For the tysonite-type anion-deficient solid solutions a. c. ionic conductivity, TSPC and DL data reveal the conductivity activation enthalpies to be solute invariant for $0.012 \leqq x \leqq 0.105$. T_{max} of the space charge peak in the TSDC spectra is found to be about 130 K for all compositions. Thermal depolarization studies reported thus far have not explored Equation (11) in a comparison of a. c. ionic conductivity and TSDC-space charge relaxation.

5. – CONCLUDING REMARKS

The study of localized ionic motions in dilute and concentrated fluorite and tysonite-type solid solutions with the TSDC technique provides detailed information on the mechanisms of ionic conductivity in these solid solutions.

The transport-structure relations can be studied down to about 5 K. Such low temperatures are a prerequisite, if reorientation processes in (222)-clusters and of (212) clusters are to be unraveled.

Besides, in the TSPC mode diffusive motions can be studied down to very low temperatures.

6. – ACKNOWLEDGEMENT

The author is grateful to Dr. M. Ouwerkerk for criticaly reading the manuscript. This work is partly based on theses investigations of Drs. K.E.D. Wapenaar, A. Roos, and M. Ouwerkerk.

REFERENCES

[1] K. E. D. WAPENAAR and J. SCHOONMAN, *J. Electrochem. Soc.*, 1979, **126**, p. 667.
[2] K. E. D. WAPENAAR, *J. Phys.*, (Paris), 1980, **41**, C 6-220.
[3] K. E. D. WAPENAAR, J. L. VAN KOESVELD and J. SCHOONMAN, *Solid State Ionics*, 1981, **2**, p. 145.
[4] J. M. RÉAU and J. PORTIER, In *Solid Electrolytes*, P. HAGENMULLER and W. VAN GOOL Eds, Academic Press, New York, 1978, p. 313.
[5] C. R. A. CATLOW, *Comments Solid State Phys.*, 1980, **9**, p. 157.
[6] C. R. A. CATLOW, J. D. COMINS, F. A. GERMANO, R. T. HARLEY, W. HAYES and I. B. OWEN, *J. Phys.*, 1981, **C. 14**, p. 329.
[7] M. OUWERKERK, E. M. KELDER, J. SCHOONMAN and J. C. VAN MILTENBURG, *Solid State Ionics*, 1983, **9/10**, p. 531.
[8] A. SHER, R. SOLOMON, K. LEE and M. W. MULLER, *Phys. Rev.*, 1966, **144**, p. 593.
[9] R. SOLOMON, A. SHER and M. W. MULLER, *J. Appl. Phys.*, 1966, **37**, p. 3727.
[10] T. TAKAHASHI, H. IWAHARA and T. ISHIKAWA, *J. Electrochem. Soc.*, 1977, **124**, p. 280.
[11] G. A. JAROSZKIEWICZ and J. H. STRANGE, *J. Phys. (Paris)*, 1980, **41**, C 6-246.
[12] J. SCHOONMAN, G. OVERSLUIZEN and K. E. D. WAPENAAR, *Solid State Ionics*, 1980, **1**, p. 211.
[13] J. R. IGEL, M. C. WINTERSGILL, J. J. FONTANELLA, A. V. CHADWICK, C. G. ANDEEN and V. E. BEAU, *J. Phys.*, 1982, **C 15**, p. 7215.
[14] A. ROOS, F. C. M. VAN DE POL, R. KEIM and J. SCHOONMAN, *Solid State Ionics*, 1984, **13**, p. 191.
[15] C. BUCCI and R. FIESCHI, *Phys. Rev. Letters*, 1964, **12**, p. 16.
[16] E. LAREDO, M. PUMA and D. R. FIGUEROA, *Phys. Rev.*, 1979, **B 19**, p. 2224.
[17] G. PFISTER and A. ABKOWITZ, *J. Appl. Phys.*, 1974, **45**, p. 1001.
[18] E. LAREDO, M. PUMA, N. SUAREZ and D. R. FIGUEROA, *Phys. Rev.*, 1981, **B. 23**, p. 3009.
[19] A. ROOS, M. BUIJS, K. E. D. WAPENAAR and J. SCHOONMAN, *J. Phys. Chem. Solids*, 1985, **46**, p. 645, 655.
[20] B. P. M. LENTING, J. A. J. NUMAN, E. J. BIJVANK and H. W. DEN HARTOG, *Phys. Rev.*, 1976, **B 14**, p. 1811.
[21] R. D. SHELLY and G. R. MILLER, *J. Solid State Chem.*, 1970, **1**, p. 218.
[22] D. Y. WANG and A. S. NOWICK, *Solid State Ionics*, 1981, **5**, p. 551.
[23] K. E. D. WAPENAAR, H. G. HOEKKOEK and J. VAN TURNHOUT, *Solid State Ionics*, 1982, **7**, p. 225.
[24] M. PUMA, A. BELLO, N. SUAREZ and E. LAREDO, *Phys. Rev.*, **B**, 1986, in press.
[25] A. B. LIDIARD, In *Handbuch der Physik*, S. FLÜGGE Ed., Springer-Verlag, Berlin, 1957, **20**, p. 246.
[26] F. K. FONG, *Progr. Solid State Chem.*, 1967, **3**, p. 135.
[27] F. A. KRÖGER and H. J. VINK, *Solid State Phys.*, 1956, **3**, p. 307.
[28] W. HAYES Ed., *Crystals with the fluorite structure*, Clarendon Press, Oxford, 1974.
[29] J. SCHOONMAN, *Solid State Ionics*, 1980, **1**, p. 121.
[30] J. H. CRAWFORD and G. E. MATTHEWS, *Semi-cond. Insulators*, 1977, **2**, p. 213.

[31] C. R. A. CATLOW, J. D. COMINS, F. A. GERMANO, R. T. HARLEY and W. HAYES, *Phys. Letters*, 1979, **71 A**, p. 97.
[32] P. W. M. JACOBS and S. H. ONG, *J. Phys. Chem. Solids*, 1980, **41**, p. 431.
[33] A. K. CHEETHAM, B. E. F. FENDER and M. J. COOPER, *J. Phys.*, 1971, **C. 4**, p. 3107.
[34] J. K. KJEMS, N. H. ANDERSEN, J. SCHOONMAN and K. CLAUSEN, *Physica*, 1983, **120 B**, p. 357.
[35] N. H. ANDERSEN, K. CLAUSEN and J. K. KJEMS, In *Transport-Structure Relations in Fast Ion and Mixed Conductors*, F. W. POULSEN, N. H. ANDERSEN, K. CLAUSEN, S. SKAARUP and O. T. SØRENSEN Eds, *Risφ National Lab.*, 1985, p. 171.
[36] N. H. ANDERSEN, K. CLAUSEN and J. K. KJEMS, *Solid State Ionics*, 1983, **9-10**, p. 543.
[37] M. OUWERKERK, F. F. VELDKAMP, N. H. ANDERSEN and J. SCHOONMAN, *Solid State Ionics*, 1985, **16**, p. 125.
[38] C. R. A. CATLOW, *J. Phys.*, 1976, **C. 7**, p. 1845.
[39] C. R. A. CATLOW, A. V. CHADWICK, G. N. GREVES and L. M. MORONEY, *Nature*, 1984, **312**, p. 601.
[40] C. G. ANDEEN, J. J. FONTANELLA, M. C. WINTERSGILL, P. J. WELCHER, R. J. KIMBLE and G. E. MATTHEWS, *J. Phys.*, 1981, **C. 14**, p. 3557.
[41] J. CORISH, C. R. A. CATLOW, P. W. M. JACOBS and S. H. ONG, *Phys. Rev.*, 1982, **B 25**, p. 6425.
[42] P. J. BENDALL, C. R. A. CATLOW, J. CORISH and P. W. M. JACOBS, *J. Solid State Chem.*, 1984, **51**, p. 159.
[43] S. F. MATAR, J. M. RÉAU, P. HAGENMULLER and C. R. A. CATLOW, *J. Solid State Chem.*, 1984, **52**, p. 114.
[44] M. OUWERKERK, *Thesis*, Utrecht University, 1986.
[45] J. SCHOONMAN, *Solid State Ionics*, 1981, **5**, p. 71.
[46] M. OUWERKERK and J. SCHOONMAN, *Solid State Ionics*, 1986, in press.
[47] I. V. MURIN and A. V. GLUMOV, *Russ. J. Phys. Chem.*, 1982, **56**, p. 660.
[48] A. ROOS, D. R. FRANCESCHETTI, M. BUIJS and J. SCHOONMAN, In *Solid State Chemistry*, 1982, R. METSELAAR, H. J. M. HEIJLIGERS and J. SCHOONMAN Eds, Elsevier, Amsterdam, 1983, p. 235.
[49] A. KESSLER, R. HÖGER and I. V. MURIN, *Mat. Res. Bull.*, 1981, **16**, p. 1185.
[50] A. ROOS, *Thesis*, Utrecht University, 1983.
[51] J. J. FONTANELLA, M. C. WINTERSGILL, P. J. WELCHER, A. V. CHADWICK and C. G. ANDEEN, *Solid State Ionics*, 1981, **5**, p. 585.
[52] C. P. SMYTH, *Dielectric Behaviour and Structure*, McGraw-Hill, New York, 1955.
[53] J. VANDERSCHUEREN and J. CASIOT, In *Thermally Stimulated Relaxation in Solids*, Topics in Applied Physics, Vol. 37, P. BRÄULICH Ed., Springer-Verlag, Berlin, 1979, p. 135.
[54] D. R. FRANCESCHETTI and P. C. SHIPE, *Solid State Ionics*, 1984, **11**, p. 285.
[55] A. F. AALDERS, A. F. M. ARTS and H. W. DE WIJN, *Solid State Ionics*, 1986, in press.
[56] C. HONG and D. E. DAY, *J. Appl. Phys.*, 1979, **58**, p. 5352.

(Received June 17, 1986.)